Guided Diffusion Monte Carlo: A Method for Studying Molecules and Ions That Display Large Amplitude Vibrational Motions

Jacob M. Finney, Ryan J. DiRisio, and Anne B. McCoy*

Department of Chemistry, University of Washington, Seattle, WA 98195

E-mail: abmccoy@uw.edu

Phone: 206-543-7464

Abstract

Diffusion Monte Carlo provides an effective and efficient approach for calculating ground sate properties of molecular systems based on potential energy surfaces. The approach has been shown to require increasingly large ensembles when intra- and intermolecular vibrations are weakly coupled. We recently proposed a guided variant of diffusion Monte Carlo to address these challenges for water clusters [J. Phys. Chem. A 2019, 123, 8063-8070. In the present study, we extend this approach and apply it to more strongly bound molecular ions, specifically CH_5^+ and $\mathrm{H}^+(\mathrm{H}_2\mathrm{O})_{n=1-4}.$ For the protonated water systems, we show that the guided DMC approach that was developed for studies of $(H_2O)_n$ can be used to describe the OH stretches and HOH bends in the solvating water molecules, as well as the free OH stretches in the hydronium core. For the hydrogen bonded OH stretches in the H_3O^+ core of $H^+(H_2O)_n$ and the CH stretches in CH_5^+ , we develop adaptive guiding functions based on the instantaneous structure of the ion of interest. Using these guiding functions, we demonstrate that we are able to obtain converged zero-point energies and ground state wave functions using ensemble sizes that are as small as 10% the size that is needed to obtain similar accuracy from unguided calculations.

Introduction

Developing and implementing general approaches for solving the Schrödinger equation for vibrational systems is a long-standing challenge in theoretical spectroscopy. For molecules and ions where the vibrations are weakly coupled and the wave functions for the states of interest are localized in a single minimum in the potential energy surface, methods based on a harmonic treatment can provide a good starting point for more sophisticated methods. These include vibrational perturbation theory, 1,2 or vibrational self-consistent field (VSCF)-based approaches, 3,4 and extensions built off of these approaches. Such approaches have been extended to studies of molecular clusters, for example $(H_2O)_n$, in which the Hamiltonian based on the intramolecular degrees of freedom is solved for a fixed cluster geometry. The situation becomes more challenging when the molecular system of interest displays large amplitude vibrations, which allow it to sample multiple minima on the potential surface even in the vibrational ground state. Additional complications emerge when these large amplitude vibrations are strongly coupled to other vibrational degrees of freedom.

A method that circumvents many of these challenges is diffusion Monte Carlo (DMC).^{7–12} In this approach, a large ensemble of localized functions, called walkers, is used to provide a Monte Carlo sampling of the ground state wave function. The coordinates and the relative weights of the walkers are propagated based on the imaginary-time time-dependent Schrödinger equation. The long time, equilibrated ensemble obtained from this propagation provides a Monte Carlo sampling of the ground state wave function of the system of interest. The associated zero-point energy is obtained by imposing the requirement that the amplitude of the wave function does not change during the propagation.

The DMC approach has been used with great success to study a broad range of molecular systems that would have been very challenging to study by approaches that rely on a basis set to expand the wave functions. $^{13-16}$ An example of such a molecule is CH_5^+ . The ground state wave function of this ion has amplitude at the 120 symmetry equivalent minima on the potential surface as well as near the 180 saddle points that connect these minima. 17,18

At the same time, the harmonic CH stretch frequencies span the range of roughly 2500 to 3300 cm^{-1} at each of the three low-energy stationary point structures. ¹⁹ This indicates that the frequency of the CH stretch is sensitive to its environment within the ion. Similarly, the frequencies of the water-bound OH bonds in protonated water clusters, $H^+(H_2O)_n$, are sensitive to their environments. This is reflected in the breadth of the features in the vibrational spectrum that are assigned to this motion in various size-selected protonated water clusters. ²⁰ The structures and frequencies of water molecules that make up a water cluster, $(H_2O)_n$, also show sensitivities to the structure of the cluster, although the couplings between the intra- and intermolecular vibrations are weaker in this case compared to the protonated water clusters. ²¹

In the case of the neutral water clusters, Mallory and Mandelshtam showed that very large ensembles of walkers were required to obtain reliable results using standard DMC approaches. For example, in their study of $(H_2O)_6$, they used an ensemble in excess of 10^6 walkers, run for 8.8×10^4 time steps.²² In DMC simulations the potential energy of each walker needs to be evaluated at each time step. As potential functions become more accurate, they often also become more expensive to evaluate. Thus, these requirements of large ensembles to obtain accurate results make the DMC approach prohibitive, and limits the size and types of systems that can be studied using DMC.

As we explored the origins of this behavior, ^{12,23} we concluded that these challenges of applying DMC to studies of neutral water clusters reflected the fact that the shifts in the frequencies of the OH stretching vibrations with the environment were comparable in size to the frequencies of the low-frequency vibrations in these clusters. Additionally, when all degrees of freedom are included in the calculation, the instantaneous equilibrium structure of the cluster as a function of the intermolecular degrees of freedom is sensitive to the precise OH bond lengths and HOH angles of the individual water molecules that make up the cluster. The need for a very large ensemble to converge this calculation reflects difficulties in sampling both the intermolecular and intramolecular degrees of freedom effectively. An

additional complication arises from the fact that the time step used in the simulation needs to be chosen based on the shortest vibrational period in the system. At the same time the simulation needs to be run long enough to sample the motions in the degrees of freedom that are associated with the low-frequency vibrations. These considerations contributed to the very large ensemble sizes Mallory and Mandelshtam found they needed to fully sample the ground state of water clusters.

On the other hand, while the above considerations make these clusters particularly challenging for DMC calculations, they represent a situation for which an adiabatic separation of the low- and high-frequency vibrations provide a good zero-order description of the vibrational dynamics. ^{6,24} In this approach, rather than focusing on the instantaneous values of the intramolecular degrees of freedom that are associated with the high frequency vibrations, the potential that is used to study the intermolecular vibrations is the average of the full potential over the probability amplitude associated with the wave function that describes the high frequency vibrations. More specifically, the vibrational energy and wave function associated with the intramolecular degrees of freedom are obtained using the potential evaluated at an instantaneous cluster geometry. Taken together, these energies are used to construct an adiabatic potential where the energy dependence on the intermolecular degrees of freedom reflects the vibrationally averaged behavior of the high frequency modes rather than their instantaneous values. Such an approach expressed in this form would be challenging for studies of such clusters using DMC, as each potential energy evaluation for the intermolecular degrees of freedom would require averaging the full potential over the ground state wave function in the intramolecular vibrations. Additionally, such a treatment would render the results of the calculation at best approximate, removing one of the attractive features of DMC, e.g. its use for obtaining an exact description of the ground state wave function, and the associated zero-point energy of the system of interest.

In a recent pair of studies, ^{12,23} we demonstrated that we could achieve a similar separation of time scales using DMC through the introduction of carefully developed guiding functions,

 Ψ_T . We applied the approach to studies of water clusters and demonstrated an order of magnitude saving in ensemble sizes used for the simulations without a loss of accuracy. Specifically, for water clusters, these guiding functions were expressed as direct products of the solutions to one-dimensional cuts through the potential surface of an isolated water molecule along each of the two OH stretch coordinates along with a harmonic description of the bend. The introduction of the guiding function in the DMC calculation has the effect of replacing the potential function with the local energy,

$$E_{\rm L} = \frac{H\Psi_T}{\Psi_T} \tag{1}$$

Our choice for Ψ_T has the effect of reducing the dependence of $E_{\rm L}$ on the intramolecular degrees of freedom compared to that of the full potential function. For example, if the OH stretch component exactly matched that of one of the OH oscillators of the water molecule in the cluster then for that cut through the potential, the local energy is constant, and the average value of the local energy for that coordinate is independent of how the walkers sample that coordinate. By removing the dependence of the local energy on the high frequency vibrations, $E_{\rm L}$ in Eq. 1 resembles an adiabatic potential that only depends on the intermolecular coordinates. Further by expressing the trial wave functions as direct products of one-dimensional wave functions, the evaluation of the $E_{\rm L}$ does not have a significant impact on the overall expense of the DMC calculation. On the other hand, the introduction of $E_{\rm L}$ does not introduce any approximations to the treatment of the ground state wave function. By removing the dependence of $E_{\rm L}$ on the OH bond lengths and HOH bend angles we found that we could realize substantial savings due to the ability to use much smaller ensemble sizes.

This approach differs from earlier studies on hydrogen clusters²⁵ and H_5^+ , ²⁶ which used normal mode descriptions for all of the vibrational degrees of freedom. Since the normal modes are evaluated for a reference structure, such an approach makes it difficult to describe systems that have multiple low-energy minima on the potential, as a Ψ_T that is based on

one of minima may not provide a good description of the ground state wave function near other minima. By focusing the trial wave function on only the high frequency vibrations, we remove this bias from our sampling at the expense that we are only describing a subset of the degrees of freedom. Such an approach was shown to work quite well for the $(H_2O)_6$ cluster in which there are several low-energy minima on the potential.²³

In the present study, we explore whether a similar strategy could be used to study protonated water clusters and CH₅⁺ for which the equilibrium OH or CH bond lengths depend strongly on the values of the coordinates associated with the low-frequency vibrations. For example, although the five CH bonds in CH₅⁺ are equivalent once zero-point energy is considered, the equilibrium CH bond lengths in the coordinates of the three lowest energy stationary points on the potential energy surface range from 1.09 to 1.2 Å. This range is comparable to the width associated with the ground state probability amplitude for a CH oscillator with a frequency of 3000 cm⁻¹, which is 0.17 Å. Likewise the frequency of the shared proton OH stretch in protonated water clusters $(H^+(H_2O)_n)$ can vary between 1000 and 2700 cm $^{-1}$ when n=2 and 4, respectively. As such, the approach for describing Ψ_T that proved to be effective for the neutral water clusters will not be as effective for these motions. Instead, we propose an approach that allows the maximum in the wave function that describes the CH or OH vibrations to depend on the environment of the CH or OH oscillator. In the case of the OH stretches in the protonated water systems, the width of the trial wave function is also allowed to adjust based on the environment. This approach will be applied to CH_5^+ and protonated water clusters to explore the savings that can be achieved as well as insights into couplings of the intermolecular and intramolecular vibrations in these ions.

Theory

Diffusion Monte Carlo and our implementation have been described elsewhere. ^{7-9,11,12,27} As outlined above, in this approach the ground state wave function for the system of interest, Φ_0 , is modeled by an ensemble of $N_{\rm W}$ localized functions, $g(\mathbf{x}; \mathbf{x}_i(\tau))$. The position of each of the walkers, $\mathbf{x}_i(\tau)$, is allowed to evolve as the wave function is propagated in imaginary time, $\tau = it/\hbar$, based on the imaginary-time time-dependent Schrödinger equation.

$$\Phi_0(\tau + \Delta \tau) = \exp\left[-(H - V_{\text{ref}})\Delta \tau\right] \Phi_0(\tau)$$

$$\approx \exp\left[-(V - V_{\text{ref}})\Delta \tau\right] \exp\left[-T\Delta \tau\right] \Phi_0(\tau) \tag{2}$$

where

$$V_{\text{ref}} = \frac{\sum_{i=1}^{N_{\text{W}}} w_i(\tau) V(x_i)}{\sum_{i=1}^{N_{\text{W}}} w_i(\tau)} - \alpha \ln \left[\frac{\sum_{i=1}^{N_{\text{W}}} w_i(\tau)}{\sum_{i=1}^{N_{\text{W}}} w_i(\tau = 0)} \right]$$
(3)

is introduced to ensure that the sum of the w_i values remains constant throughout the simulation. In the above expression, w_i represents the relative weight of each of the walkers in the ensemble, $\alpha = 0.5/\Delta \tau$, and $N_{\rm W}$ represents the total number of walkers that make up the ensemble. With this constraint, the time-averaged value of $V_{\rm ref}$ gives the zero-point energy of the system of interest once the system has equilibrated. While the action of the kinetic contribution to the propagator shifts the values of the components \mathbf{x}_i at each time step,

$$w_i(\tau + \Delta \tau) = \exp\left[-(V(\mathbf{x}_i(\tau)) - V_{\text{ref}})\Delta \tau\right] w_i(\tau)$$
(4)

adjusts the contribution of each walker to the ensemble based on its energy. A branching step is introduced at each time step in the simulation to ensure that all of the walkers contribute to the ensemble and that the weights do not localize on a small fraction of the walkers. In this step, an equal number of walkers with large and small weights is identified. This set of walkers includes all of the walkers for which $w_i(\tau) > 20$ or $w_i(\tau) < 0.1$. The small-weight walkers are then removed from the ensemble, while each of the large-weight walkers is duplicated, and each member of the new pair of walkers is given a weight that is half the value of the weight of the duplicated walker. Once equilibrated, a snapshot of $\Phi_0(\tau)$ at any time τ provides the ground state wave function.

The above description focuses on what we will refer to as unguided DMC simulations. In the guided approach, rather than using DMC to obtain Φ_0 , we use the ensemble of walkers to evaluate f, where 10,28

$$f = \Psi_T \Phi_0 \tag{5}$$

and $V(\mathbf{x}_i)$ in Eq. 3 is replaced by the local energy, $E_{\rm L}$ defined in Eq. 1. As mentioned above, in this study, Ψ_T is the product of one-dimensional wave functions that are each functions of one of the high frequency intramolecular coordinates, e.g. an XH bond length or an HOH angle. These guiding functions will be described in the following section.

In order to obtain projections of the probability amplitude onto coordinates of interest we use a technique called descendent weighting.^{9,29} Specifically, evaluation of the probability amplitude, Φ_0^2 , from f requires multiplication of f by Φ_0/Ψ_T . Suhm et al. and Barnett et al. have shown that

$$\frac{\Phi_0(\mathbf{x}_i(\tau))}{\Psi_T(\mathbf{x}_i(\tau))} \propto \frac{w_i(\tau + \delta \tau)}{w_i(\tau)} \tag{6}$$

where $w_i(\tau + \delta \tau)$ represents the weight of the *i*th walker after it has been propagated forward by $\delta \tau$.

Numerical details

For the simulations of the protonated water clusters, $H^+(H_2O)_{n=2,3,4}$ the potential used to propagate the walkers was developed by Yu and Bowman. 16 The version of this potential used in this study incorporates an updated three-body term involving the hydronium core and two water molecules. We needed to use this modified surface because preliminary studies using the previously reported surface has a low-energy region that corresponds to dissociation of H⁺ from the water cluster, which was sampled by our continuous weight simulations. The potential energy surface for H₃O⁺ is the one developed by Huang, Carter, and Bowman.³⁰ The simulations for the protonated water clusters were first equilibrated by running for 5000 time steps with a $\Delta \tau$ of 10 a.u. without the use of a guiding function, then the simulations were run for an additional 20 000 time steps with a $\Delta \tau$ of 1 a.u. either with or without a guiding function. This added equilibration step was introduced to ensure that the potential energy surface was fully sampled at the beginning of the simulation. Simulations with a $\Delta \tau$ of 10 a.u. were run for 20 000 time steps without this added equilibration step. The zeropoint energy was then obtained by time averaging $E_{\rm ref}$ over the final 15 000 time steps of the simulation. Although the simulations that are run using the 10 a.u. time steps are allowed to propagate for roughly three times as long as the simulations that use the 1 a.u. time step, we find that the average zero-point energies obtained when we perform the averages over the same propagation times as are used to analyze the 1 a.u. results agree with those obtained using longer propagation times, albeit with larger statistical uncertainties.

For the calculations involving CH₅⁺ and its deuterated analogues, the initial ensemble of walkers is distributed randomly among the 120 equivalent minima on the potential energy surface. For these calculations we use the potential of Jin, Braams, and Bowman, which was fit to electronic energies of CH₅⁺ calculated at the CCSD(T)/aug-cc-pVTZ level of theory/basis. ¹⁹ Each simulation was run for 20 000 time steps with a $\Delta\tau$ of 1 a.u. The zero-point energy was obtained by time averaging $E_{\rm ref}$ from 5000 time steps to the end of the simulation. This allows us to ensure that the ensemble is equilibrated before the energies

are collected.

All of the reported energies are based on five independent simulations, and the uncertainties represent one standard deviation based on these values, while descendant weights were collected 20 times for 250 time steps over the last 15 000 time steps in order to collect wave functions for each simulation.

For the guided simulations, the HOH bends were described by harmonic oscillators based on a harmonic frequency of 1668 cm⁻¹ and a G-matrix element³¹ of 2.338 amu⁻¹ Å⁻².²³ The wave functions that describe the CH bonds in CH₅⁺ and the OH bonds in the protonated water clusters were obtained using a discrete variable representation (DVR)³² based on one-dimensional slices through the potentials of interest. Descriptions of these calculations, and the resulting wave functions are provided in the Supporting Information. The resulting wave functions were interpolated using a cubic spline. Calculations of the drift term and local energy require the first and second derivatives of Ψ_T with respect to the Cartesian coordinates. These derivatives were evaluated numerically using a three-point finite difference.

Results

$$\mathbf{H}^+(\mathbf{H}_2\mathbf{O})_n$$

Protonated water clusters, like neutral water clusters, present challenges for DMC approaches. The smallest of these ions, H_3O^+ , is covalently bound, and the OH stretch frequencies are 3445 and 3536 cm⁻¹, ³⁰ which is about 200 cm⁻¹ lower than the OH stretch frequencies in an isolated water molecule. The next smallest system, $H^+(H_2O)_2$, shows large amplitude vibrations and large couplings between high and low frequency vibrations. These stronger couplings result from the very low frequency of the shared proton stretch, ≈ 1000 cm⁻¹, which is strongly coupled to the stretching and bending vibrations of the terminal water molecules. ^{27,33} As we add more water molecules, the amplitude of the water-bound OH stretching vibrations in the hydronium core are intermediate between H_3O^+ and $H^+(H_2O)_2$,

and the frequencies of these vibrations in $H^+(H_2O)_3$ and $H^+(H_2O)_4$ are approximately 2100 and 2653 cm⁻¹, respectively. ^{34,35}

As we consider which vibrational degrees of freedom to include in the guiding functions, several options emerge. Given recent successes in applying a similar approach to studies of neutral water clusters, 12,23 one option is to use a direct product of wave functions that describe the OH stretch and HOH bends in the terminal water molecules as well as the vibrations of the OH stretches in the hydronium core that are not bound to water molecules. For these vibrations, we use the ground state wave functions obtained for an isolated water molecule. 36 Since the water bound OH stretches in the hydronium core of $H^+(H_2O)_n$ display a broad range of frequencies, it is not likely that the same distribution can be used to describe the ground state wave function of this oscillator in all of the possible structures of these systems. As we consider the development of the guiding functions to use for these systems, we focus on functional forms that are transferable to larger protonated water clusters, and which do not presume a specific bonding configuration.

We start by considering the convergence behavior of guided and unguided DMC calculations for H₃O⁺. The results of this analysis are shown in panel A of Figure 1. In all of the panels in this figure, the red symbols and lines provide the results of unguided DMC calculations with a time step of 1 a.u., while the gold lines and symbols provide the results when the guiding functions based on the OH stretches in an isolated water molecule are used to describe all of the unbound OH stretches in the hydronium core, and the OH stretches in the solvating water molecules. In addition, the guiding functions include a harmonic description of the HOH bend in the solvating water molecules. We do not try to describe the HOH bends in the hydronium core with the guiding functions due to redundancies in these coordinates in planar geometries. To aid in comparisons, the results based on the guided DMC calculation using the largest ensemble are extended using a dotted line, and the uncertainties are shown with shading of the same color. For hydronium, both the guided and unguided approaches yield results that are in good agreement with the previously reported

DMC ground state energy of 7453 cm^{-1} , which was obtained using an unguided simulation with 20 000 walkers and a 1 a.u. time step. ³⁷ For the unguided calculations, ensembles larger than 10 000 walkers yield energies that are well-converged, while for the guided calculations, 1000 walkers are needed to achieve similar accuracy. These results are consistent with our earlier studies of water clusters. Unlike the study of water clusters, in which the trial wave function was chosen to provide a good description of the OH stretch in water, here we use the water-based OH wave function to describe the OH stretches in H_3O^+ . We have also performed these calculations using guiding functions based on the ground state wave function for an OH stretch in H_3O^+ and obtain results that are nearly identical to those reported in Figure 1A (see Table S1).

A similar approach was applied to calculations of the zero-point energies of $H^+(H_2O)_n$ for n=2, 3 and 4, and the results are shown with the red and gold symbols and lines in panels B, C and D of Figure 1. For n=2, shown in panel B, the energies obtained using the guided DMC approach do not change significantly when 500 or 5000 walkers are used, although the uncertainties of the results decrease as larger ensembles are used. For the unguided simulations, 10 000 walkers are needed to achieve similar results. These results are about 20 cm⁻¹ lower than previously reported zero-point energies for this ion, 12 393 (5). The difference reflects small differences in the potential surface used here, which is based on the potential for larger protonated water clusters, developed by Yu and Bowman. Similar improvements in performance are found for the clusters with three and four water molecules, shown with red and gold symbols and lines in panels C and D of Figure 1.

For $H^+(H_2O)_3$, both the guided and unguided DMC calculations give a zero-point energy of roughly 18 000 cm⁻¹ while for the guided simulations this result is achieved with as few as 2000 walkers, at least 20 000 walkers are required to obtain this energy using the unguided approach. In both cases the uncertainties are uncomfortably large. The energies are within 5 cm^{-1} of the converged zero-point energy when 10 000 walkers for the guided calculation and 100 000 are required to obtain similar accuracy from the unguided calculations.

In the case of $H^+(H_2O)_4$, the guided DMC simulations give a zero-point energy of 23 409 (6) cm⁻¹ when 30 000 walkers are used. The unguided simulations give an energy of 23 421 (10) cm⁻¹ when 100 000 walkers were propagated using a 1 a.u. time step. This energy is 11 cm⁻¹ above the energy obtained using the guided approach. For comparison, when we perform large unguided simulations with a larger 10 a.u. time step we obtain a zero-point energy of 23 397 (4) cm⁻¹, which is in very good agreement with the guided results. The convergence behavior for $H^+(H_2O)_4$ is similar to the behavior we noted for $(H_2O)_6$ in a recent study.²³ As in that work, significantly larger ensembles are required for the unguided simulations than for the guided ones. In the case of $(H_2O)_6$, 1 000 000 walkers were needed to obtain accurate zero-point energies using unguided DMC approaches.^{23,39} In that work, we also found that the large unguided calculations that employed the 1 a.u. time step appeared to be converging to an energy that was larger than the value obtained from the guided DMC calculations.

We can also compare the zero-point energies obtained by the guided DMC approach to the value obtained when 20 000 walkers are used, in an unguided simulation with a 10 a.u. time step. For $H^+(H_2O)_3$, the calculation with this larger time step appears to be converged at this ensemble size, and nearly identical zero-point energies are obtained when 25 000 or 15 000 walkers are used. In these cases, the calculated energy agrees with the values obtained from unguided simulations with ensembles of 40 000 or more walkers when the 1 a.u. time step was used. In the case of $H^+(H_2O)_4$, the DMC simulation with 20 000 walkers and a 10 a.u. time step gives a zero-point energy of 23 441 (8) cm⁻¹, which is 32 cm⁻¹ higher than the value obtained using the guided approach. When we increase the ensemble size used for the unguided simulation to 75 000 walkers, the agreement between the energy calculated by this approach is in excellent agreement with the values obtained using the guided approach. As with $(H_2O)_6$, the larger time step compensates for sampling issues. While the total propagation times for the 1 a.u. and 10 a.u. simulations differ, if we evaluate the results of the 10 a.u. simulations using the same propagation times used for the

1 a.u. ones, the energies do not change significantly, but the uncertainties are larger when the smaller amount of propagation time is used (see Tables S2 to S4).

One concern with using smaller ensemble sizes in the DMC simulations is that the potential may not be as well-sampled. To explore the effect of ensemble size on the description of the wave function, we focus on the OOO bend angle in $H^+(H_2O)_3$. We choose this angle because earlier work exploring projections of the probability amplitude for this cluster ion onto various internal coordinates indicated that this was among the most problematic. ²⁷ This can be seen in the plots of projections of the probability amplitude onto several internal coordinates based on unguided simulations with 20 000 walkers, in the left panels of Figure S1, with the projection onto the OOO angle also shown in the results reported in the upper panel of Figure 2. For these plots, we show the probability distributions obtained by projecting the probability amplitude for twenty wave functions onto the angle of interest. As is seen, while the average distribution looks reasonable (thick blue line) there are large fluctuations among the results that are obtained from the individual wave functions. This is reflected by the noisiness of the curves plotted in different colors as well as through the error bars that are shown for 110°, 120° and 130°. These large fluctuations among the results obtained using different wave functions reflect the correlation between this angle and the higher frequency HOH bend involving the bound OH bonds in the hydronium core. It also reflects changes in the optimized value of these angles as the free OH bond is displaced out of the plane of the three oxygen atoms (basically the umbrella motion of the hydronium core). When the hydronium core is planar, the optimized value of the OOO angle is close to 120°, while in the equilibrium geometry the OOO angle is closer to 113°. These couplings combined with the difference in the frequencies of these vibrations makes the projection of the ground state probability amplitude onto this coordinate difficult to capture using standard DMC approaches. Increasing the ensemble size mitigates the problem somewhat, as can be seen by comparing the size of the error bars for the curves plotted in green (40 000 walkers) and blue (20 000 walkers). The distributions from individual wave functions obtained in these calculations are provided in the middle panel of Figure S1. Interestingly, although increasing the time step used for the simulations with 20 000 walkers to 10 a.u. leads to better convergence behavior for the energy, the projections of the probability amplitudes obtained using the 10 a.u. time step with 20 000 walkers looks very similar to those reported in Figure 2A. If we compare these results to those obtained when the guided DMC approach is used with only 10 000 walkers (red curve in Figure S1B), we find that the smaller ensemble provides a further improvement to the results.

As with the neutral water clusters, the origins of the improved convergence behavior when guided DMC approaches are used can be traced to the fact that displacements of the high frequency OH stretches lead to large fluctuations in the potential energy, particularly when compared to the lower-frequency vibrations. This makes simultaneous sampling of the high and low-frequency modes less efficient. By introducing guiding functions for the high frequency vibrations, particularly the unbound OH stretches, the low-frequency motions are sampled on what is effectively an adiabatic potential surface in which the full potential has been averaged over these high frequency motions.

The question naturally arises as to whether the approach could be improved by incorporating the bound OH stretches in the hydronium core in the importance sampling scheme. As noted above, the frequency of these OH oscillators is sensitive to the bonding environment. A recent study of the effects of solvation environment on the vibrational frequencies of the bound OH stretches in the hydronium core of protonated water clusters illustrated that the frequencies of these OH oscillators can be correlated to the distance between the oxygen atoms in the hydronium core and the associated water molecule. ⁴⁰ Additionally, as with neutral water molecules, stronger hydrogen bonds are associated with both lower OH stretch frequencies and longer OH bonds in the donor hydronium molecule. In the case of $H^+(H_2O)_3$ and $H^+(H_2O)_4$, the equilibrium OH bond lengths differ by 0.025 Å, based on the potential used in this study, while the reported frequencies of these vibrations differ by roughly 550 cm⁻¹. Based on these observations, we cannot expect that the strategy of using

a single trial wave function to describe an arbitrary environment for the OH bonds in water clusters will work for the water solvated OH bonds in hydronium core.

To address the above observations and concerns, we developed a modified strategy in which we drew on the correlations between the distance between the oxygen atoms in the accepting water molecule and the donating hydronium core, and the location of the maximum and the value of the width of this OH stretch wave function. For these calculations we evaluated one-dimensional scans of the potential as a function of the OH bond length for various OO distances keeping all other coordinates in their geometries based on the equilibrium structure of the ion. Using these scans, we calculated the ground state wave function for the OH stretch using a discrete variable representation (DVR).³² The results of this analysis are provided in Figure 3, where in panel A, the maximum in the ground state wave function, $r_{\text{OH}}^{\text{max}}$ is plotted, while in panel B, we plot the width of the distribution, σ . Details of these calculations are provided in the supporting information. To obtain a trial wave function for the bound OH stretches in the hydronium core, we use the instantaneous OO distance along with the curves in Figure 3 to shift and scale the water-bound OH stretch wave function evaluated at the equilibrium geometry of the cluster.

The results that are obtained when we introduced guiding functions to describe the water bound OH stretches in the hydronium core are provided with blue and purple curves in panels C and D of Figure 1. The differences between these two sets of calculations are the parameters used to describe the wave function. For the blue curve, the parameters and reference wave function are based on $H^+(H_2O)_3$, while the parameters and reference wave function for $H^+(H_2O)_4$ are used to generate the purple curve. As the results provided in Figure 1 and Tables S2 to S4 show, the convergence properties of these calculations are very similar to those obtained when guiding functions are only used to describe the OH stretches and HOH bends of the outer water molecules and the free OH stretch in the hydronium. While at one level the lack of significant improvement in the convergence properties of the results when we incorporated trial wave functions for the bound OH stretches in the hydronium

core is disappointing, the fact that the convergence behavior has not deteriorated with the introduction of the trial wave function indicates that such a strategy should be successful as we look to larger clusters, where a single cluster displays a range of strengths of hydrogen bonded interactions.

\mathbf{CH}_{5}^{+}

We next turn our attention to CH_5^+ and its deuterated analogues. While in the water and hydronium molecules, all of the OH bonds are equivalent by symmetry, the CH bonds in CH_5^+ are not equivalent in its minimum energy structure. Specifically, for the minimum energy geometry the CH bonds range in length from 1.09 to 1.20 Å. The frequencies that are obtained from potential cuts along each of these CH distances vary from 2384 to 3070 cm⁻¹ (see Table S5 and Figure S2). On the other hand, once zero-point energy is introduced the five CH bonds become equivalent. This is due to the fact that the barriers that separate the 120 equivalent minima on the potential are lower than the zero-point energy in the low-frequency vibrations that are responsible for the isomerization. To account for this, we first consider a guiding function of the form

$$\Psi_t(\mathbf{x}) = \prod_{i=1}^5 \psi\left(r_{\mathrm{CH}}^{(i)}\right) \tag{7}$$

where $r_{\rm CH}^{(i)}$ represents the CH⁽ⁱ⁾ bond length in CH₅⁺ and ψ represents the average of five wave functions that are obtained by solving the one-dimensional Schrödinger equation using one dimensional cuts of the potential energy surface along the five CH bond lengths. The resulting wave function is plotted as a purple dotted line in Figure 4, and the wave functions that correspond to the longest (CH⁽⁵⁾) and shortest (CH⁽²⁾) CH bond lengths are plotted with red dashed and gold solid lines, respectively.

When we use the average CH stretch wave function as the trial wave function in the DMC calculations, we find that the convergence behavior of the zero-point energy is no faster than

the unguided approach. It also appears that the calculations are converging to an energy that is slightly too large. Specifically, a calculation based on 20 000 walkers yielded a zeropoint energy of 10 926(4) cm⁻¹, which is approximately 10 cm⁻¹ above the zero-point energy obtained using an unguided calculation with 20 000 walkers, 10 918(6) cm⁻¹. The reason the trial wave function provided by Eq. 7 is not appropriate for this problem is illustrated in the results provided in Figure 4. First, the 0.11 Å difference between the lengths of the CH⁽²⁾ and CH⁽⁵⁾ bonds in the minimum energy geometry means that the average wave function does not provide a very good approximation to the ground state wave function associated with either of these oscillators. This can be seen by comparing the three wave functions plotted in Figure 4A. For comparison, in a recent study of the equilibrium geometries of water clusters containing two to six water molecules, we found that these equilibrium OH bond lengths differ by at most $0.04~{\rm \AA}.^{41}$ The difficulties in using a single wave function to describe the five CH oscillators in CH_5^+ is further illustrated in a comparison of the local energy function obtained when $E_{\rm L}$ in Eq. 1 is evaluated using the potential cut along $r_{\rm CH}^{(5)}$ (solid black curve) in Figure 4B based on the three wave functions shown in panel A. When we use the average wave function to calculate the local energy it shows a sizable increase at larger values of $r_{\rm CH}$. In contrast, the local energy plotted in the red dashed line is constant as the corresponding wave function is an eigenstate of this Hamiltonian. Similar behavior is found when we calculate the local energy using a cut through the potential through $r_{\text{CH}}^{(5)}$ (panel C), although now the purple trace deviates from zero at small values of $r_{\rm CH}^{(2)}$. Based on these plots and the poor performance of guided DMC when the guiding function in Eq. 7 is used, we conclude that this approach that was effective for water clusters will not work well for CH_5^+ . On the other hand, while the value of $\langle r_{CH}^{(i)} \rangle$ depends on which CH bond is being considered, the widths of these distributions are less sensitive to the molecular environment.

To address this challenge, we need to find a procedure to relate $\langle r_{\rm CH}^{(i)} \rangle$ to the instantaneous structure of CH₅⁺, just as we correlated the position and the widths of the wave functions for the bound OH stretches in H⁺(H₂O)_n to the OO distances. It has long been recognized that

the structure of CH₅⁺ can be described as a CH₃⁺ part, in which the three CH bond lengths are roughly equal and the distances between these three hydrogen atoms are also equal, and a H₂ part, which is characterized by a shorter H-H distance. ⁴² In Tables S6-S8, for each hydrogen atom, we report the H-H distances to each of the other four hydrogen atoms, evaluated at each of the three stationary point geometries on the potential of CH₅⁺. The values based on the equilibrium structure of CH₅⁺ are also plotted as functions of the corresponding CH bond lengths in the upper panel of Figure 5. For the CH bond lengths that involve hydrogen atoms in the H₂ group, the H-H distances range from 0.95 to approximately 2 Å. These are the two longest CH bonds and the breadth of the distances is illustrated by the blue and gold distribution in Figure 5A. For the hydrogen atoms in the CH₃ group the H-H distances only range from 1.7 to 1.9 Å, as is seen in the green, red and purple distributions. Similar behavior is seen for the other stationary point geometries. Based on this observation, we find that there is a correlation between the standard deviation among the four H-H distances involving a chosen hydrogen atom to the value of $\langle r_{\rm CH}^{(i)} \rangle$, which we have plotted in panel B of Figure 5. To incorporate this observation into our trial wave function, we define

$$\Psi_T = \prod_{i=1}^5 \phi \left(r_{\text{CH}}^{(i)} - \delta(\sigma_i) \right) \tag{8}$$

where $\phi(r_{\text{CH}})$ is the wave function associated with the lowest frequency CH oscillator in the equilibrium geometry, the gold curve in Figure 4A.

To obtain σ_i , we first scale all of the CH bond lengths so they are all the same value (1 a_0), and σ is the standard deviation of the four H-H distances involving the hydrogen atom of interest. The scaling is introduced to remove the effects of changes in the instantaneous CH bond lengths on the value of σ . In Figure 5B, we plot the difference between the associated CH bond length and $r_{\rm CH}^{(2)}$ in the equilibrium geometry, δ , as a function of these scaled σ values. As is seen, δ increases monotonically with σ . We then fit this data to a shifted

exponential,

$$\delta(\sigma_i) = A \exp(B\sigma_i) + C \tag{9}$$

Using this relationship, we have allowed the trial wave function to account for variations in the equilibrium CH bond length on the structure of the ion while keeping all of the hydrogen atoms equivalent. This does not add significant complexity to the DMC calculation.

The results of guided (blue) and unguided (red) DMC calculations of the ground states of CH_5^+ , CD_5^+ , and $CH_3D_2^+$ are provided in Figure 6 for various ensemble sizes. As is seen, in all of the isotopologues, when 2000 to 5000 walkers are used in the unguided simulations, the energies and associated uncertainties are comparable to the values obtained from unguided simulations with 20 000 walkers. Both values are also in good agreement with previously reported zero-point energy for this potential energy surface (black line with grey shading). ¹⁹

In addition to confirming that the procedure is effective, these calculations also allowed us to explore the transferability of the trial wave functions with partial deuteration. The only change in Ψ_T in Eq. 8 when one or more of the hydrogen atoms are replaced with deuterium is the trial wave function that is used is the one appropriate for the ground state of the CD stretch based on the potential cut along $r_{\text{CH}}^{(2)}$. We also explored how well this wave function performs on the various deuterated isotopologues of CH_5^+ . One interesting feature of partially deuterated forms of CH_5^+ is that the probability amplitude becomes localized in a subset of the 120 minima on the potential. This localization reflects differences among the zero-point energies of the CH vibrations in the various bonding environments, as is illustrated by the wave functions plotted in Figure S2.

Overall, the agreement between the results of these calculations and previously reported zero-point energies for CH_5^+ is very good, further validating the approach. In the cases of CH_4D^+ and $CH_3D_2^+$ the energies obtained in the present study are between five and ten cm^{-1} higher than previously reported values based on both guided and unguided calculations. These differences are likely due to difficulties in sampling the high frequency CH stretches when a 10 a.u. time step is used, as was done in the previous studies of CH_5^+ . Studies of

water monomer showed that the use of a 10 a.u. time step in DMC calculations resulted in zero-point energies that are about five cm⁻¹ lower than the zero-point energy obtained from a converged variational calculation. 23,43 Interestingly, for D₂O the 10 a.u. time step provided an accurate value for the zero-point energy. The fact that we get slightly different zero-point energies when we reduce the time step from 10 a.u. to 1 a.u. for only CH₄D⁺ and CH₃D₂⁺ likely reflects fact that these are the mixed isotoplogues that have more hydrogen atoms than deuterium atoms.

Conclusions

In this study, we have demonstrated that the guided DMC approach, which we recently developed for studies of water clusters, 12,23 can be used to study systems where the form of the vibrational wave function that describes the XH stretches depends on the local environment experienced by that bond. We applied the approach to studies of protonated water clusters with four or fewer water molecules and to CH_5^+ . We showed that we could obtain substantial savings in the computational demands of the DMC simulations for these systems, in some cases as much as an order of magnitude, compared to unguided simulations. We also showed that the wave functions obtained from these smaller ensembles resulting from guided simulations were better converged than the wave functions obtained using unguided approaches with substantially larger ensemble sizes.

By being able to converge the zero-point energies and wave functions with smaller ensembles, we were able to show that for the protonated water systems, the ensemble sizes used in previous studies are likely not large enough to obtain accurate ground state properties. 15,16 With the approach validated and the savings that were achieved we are positioned to explore larger cluster ions, specifically $H^+(H_2O)_{5,6}$ where experimental studies have demonstrated that multiple isomers are sampled in the low-temperature experiments, and the most stable forms appear to be affected by partial deuteration. 40,44 The ability to separate the CH

stretch vibrations from the lower frequency motions in CH_5^+ also provides an opportunity to further explore the five dimensional rotor model, which was successfully used by Schlemmer and co-workers to analyze their rotationally resolved spectrum. $^{45-47}$

Acknowledgement

Support from the Chemistry Division of the National Science Foundation (CHE-1856125) is gratefully acknowledged. We also thank Joel Bowman and his research group for providing us with the potential functions that were used in this study. Parts of this work were performed using the Ilahie cluster, which was purchased using funds from a MRI grant from the National Science Foundation (CHE-1624430). This work was also facilitated through the use of advanced computational, storage, and networking infrastructure provided by the Hyak supercomputer system and funded by the STF at the University of Washington.

Supporting Information Available

A description of the calculation of the one-dimensional OH and CH wave functions; A description of the calculations of $r_{\text{OH}}^{\text{max}}$ and σ_{OH} in Figure 3; Projections of the probability amplitude of $H^+(H_2O)_3$ onto the OOO angle, the bound HOH angle, and the outer HOH angle with and without the use of a guiding function; Ground state wave functions for the CH stretches evaluated at the three stationary point geometries of CH_5^+ ; Convergence of the zero-point energy for the deuterated analogues of CH_5^+ that are not shown in Figure 6; Tables providing the data plotted in Figures 1, 3, 6, and S3; Tables providing the wave functions used to evaluate Ψ_T for the CH stretches in CH_5^+ and the bound OH stretches in the hydronium core of $H^+(H_2O)_3$ and $H^+(H_2O)_4$.

References

- Sibert, E. L. Theoretical Studies of Vibrationally Excited Polyatomic Molecules Using Canonical Van Vleck Perturbation Theory. J. Chem. Phys. 1988, 88, 4378–4390.
- (2) Barone, V. Anharmonic Vibrational Properties by a Fully Automated Second-Order Perturbative Approach. J. Chem. Phys. 2005, 122, 014108.
- (3) Bowman, J. M. The Self-Consistent-Field Approach to Polyatomic Vibrations. *Acc. Chem. Res.* **1986**, *19*, 202–208.
- (4) R. B. Gerber, V. Buch and M. A. Ratner, Self-Consistent Field and Statistical Wavefunction Methods for Excited Vibrational States of Polyatomic Molecules. J. Chem. Phys. 1982, 77, 3022–3030.
- (5) Bowman, J. M.; Carter, S.; Huang, X. MULTIMODE: a Code to Calculate Rovibrational Energies of Polyatomic Molecules. *Int. Rev. Phys. Chem.* **2003**, *22*, 533–549.
- (6) Wang, Y.; Bowman, J. M. Ab initio Potential and Dipole Moment Surfaces for Water. II. Local-Monomer calculations of the Infrared Spectra of Water Clusters. J. Chem. Phys. 2011, 134, 154510.
- (7) Anderson, J. B. A Random-Walk Simulation of the Schrödinger Equation: H₃⁺. J. Chem. Phys. **1975**, 63, 1499–1503.
- (8) Anderson, J. B. Quantum Chemistry by Random Walk. H ${}^{2}P$, H₃⁺ D_{3h} ${}^{1}A'_{1}$, H₂ ${}^{3}\Sigma_{u}^{+}$, H₄ ${}^{1}\Sigma_{g}^{+}$, Be ${}^{1}S$. J. Chem. Phys. **1976**, 65, 4121–4127.
- (9) Suhm, M. A.; Watts, R. O. Quantum Monte Carlo Studies of Vibrational States in Molecules and Clusters. *Phys. Rep* **1991**, *204*, 293 329.
- (10) Reynolds, P. J.; Ceperley, D. M.; Alder, B. J.; Lester, W. A. Fixed-Node Quantum Monte Carlo for Molecules. J. Chem. Phys. 1982, 77, 5593–5603.

- (11) McCoy, A. B. Diffusion Monte Carlo Approaches for Investigating the Structure and Vibrational Spectra of Fluxional Systems. *Int. Rev. Phys. Chem.* **2006**, *25*, 77–107.
- (12) Lee, V. G. M.; McCoy, A. B. An Efficient Approach for Studies of Water Clusters Using Diffusion Monte Carlo. *J. Phys. Chem A* **2019**, *123*, 8063–8070.
- (13) Wang, X. G.; Carrington Jr., T. Vibrational energy levels of CH₅⁺. J. Chem. Phys. **2008**, 129, 234102.
- (14) Vendrell, O.; Gatti, F.; Meyer, H.-D. Full Dimensional (15-dimensional) Quantum-Dynamical Simulation of the Protonated Water Dimer. II. Infrared Spectrum and Vibrational Dynamics. J. Chem. Phys. 2007, 127, 184303.
- (15) Esser, T. K.; Knorke, H.; Asmis, K. R.; Schöllkopf, W.; Yu, Q.; Qu, C.; Bowman, J. M.; Kaledin, M. Deconstructing Prominent Bands in the Terahertz Spectra of H₇O₃⁺ and H₉O₄⁺: Intermolecular Modes in Eigen Clusters. J. Phys. Chem. Lett. 2018, 9, 798–803.
- (16) Yu, Q.; Bowman, J. M. Communication: VSCF/VCI Vibrational Spectroscopy of H₇O₃⁺ and H₉O₄⁺ Using High-Level, Many-Body Potential Energy Surface and Dipole Moment Surfaces. J. Chem. Phys. **2017**, 146, 121102.
- (17) Thompson, K. C.; Crittenden, D. L.; Jordan, M. J. T. CH_5^+ : Chemistry's Chameleon Unmasked. J. Am. Chem. Soc. 2005, 127, 4954–4958.
- (18) McCoy, A. B.; Braams, B. J.; Brown, A.; Huang, X.; Jin, Z.; Bowman, J. M. Ab Initio Diffusion Monte Carlo Calculations of the Quantum Behavior of CH₅⁺ in Full Dimensionality. J. Phys. Chem. A 2004, 108, 4991–4994.
- (19) Jin, Z.; Braams, B. J.; Bowman, J. M. An ab Initio Based Global Potential Energy Surface Describing $CH_5^+ \to CH_3^+ + H_2$. J. Phys. Chem. A **2006**, 110, 1569–1574.
- (20) Headrick, J. M.; Diken, E. G.; Walters, R. S.; Hammer, N. I.; Christie, R. A.; Cui, J.;

- Myshakin, E. M.; Duncan, M. A.; Johnson, M. A.; Jordan, K. D. Spectral Signatures of Hydrated Proton Vibrations in Water Clusters. *Science* **2005**, *308*, 1765–1769.
- (21) Boyer, M. A.; Marsalek, O.; Heindel, J. P.; Markland, T. E.; McCoy, A. B.; Xantheas, S. S. Beyond Badger's Rule: The Origins and Generality of the Structure-Spectra Relationship of Aqueous Hydrogen Bonds. J. Phys. Chem. Lett. 2019, 10, 918–924.
- (22) Mallory, J. D.; Brown, S. E.; Mandelshtam, V. A. Assessing the Performance of the Diffusion Monte Carlo Method as Applied to the Water Monomer, Dimer, and Hexamer. J. Phys. Chem. A 2015, 119, 6504–6515.
- (23) Lee, V. G. M.; Vetterli, N. J.; Boyer, M. A.; McCoy, A. B. Diffusion Monte Carlo Studies on the Detection of Structural Changes in the Water Hexamer upon Isotopic Substitution. *J. Phys. Chem. A* **2020**, *124*, 6903–6912.
- (24) Talbot, J. J.; Yang, N.; Huang, M.; Duong, C. H.; McCoy, A. B.; Steele, R. P.; Johnson, M. A. Spectroscopic Signatures of Mode-Dependent Tunnel Splitting in the Iodide–Water Binary Complex. J. Phys. Chem. A 2020, 124, 2991–3001.
- (25) Schmidt, M.; Constable, S.; Ing, C.; Roy, P.-N. Inclusion of Trial Functions in the Langevin Equation Path Integral Ground State Method: Application to Parahydrogen Clusters and Their Isotopologues. J. Chem. Phys. 2014, 140, 234101.
- (26) Acioli, P. H.; Xie, Z.; Braams, B. J.; Bowman, J. M. Vibrational Ground State Properties of H₅⁺ and its Isotopomers from Diffusion Monte Carlo Calculations. *J. Chem. Phys.* 2008, 128, 104318.
- (27) McCoy, A. B.; Dzugan, L. C.; DiRisio, R. J.; Madison, L. R. Spectral Signatures of Proton Delocalization in $H^+(H_2O)_{n=1-4}$ Ions. Faraday Discuss. **2018**, 212, 443–466.
- (28) B. L. Hammond, J., W. A. Lester, Reynolds, P. J., Eds. Monte Carlo Methods in Ab

- Initio Quantum Chemistry; World Scientific Lecture and Course Notes in Chemistry; World Scientific Publishing Co.: Singapore, 1994; Vol. 1.
- (29) Barnett, R.; Reynolds, P.; W.A Lester, J. Monte Carlo Algorithms for Expectation Values of Coordinate Operators. J. Comput. Phys. 1991, 96, 258 276.
- (30) Huang, X.; Carter, S.; Bowman, J. M. *Ab initio* Potential Energy Surface and Rovibrational Energies of H₃O⁺ and its Isotopomers. *J. Chem. Phys.* **2003**, *118*, 5431–5441.
- (31) Wilson, E. B.; Decius, J. C.; Cross, P. C. *Molecular Vibrations*; Dover: New York, 1955.
- (32) Colbert, D. T.; Miller, W. H. A Novel Discrete Variable Representation for Quantum Mechanical Reactive Scattering via the S-matrix Kohn Method. J. Chem. Phys. 1992, 96, 1982–1991.
- (33) Guasco, T. L.; Johnson, M. A.; McCoy, A. B. Unraveling Anharmonic Effects in the Vibrational Predissociation Spectra of H₅O₂⁺ and Its Deuterated Analogues. J. Phys. Chem. A 2011, 115, 5847–5858.
- (34) Duong, C. H.; Yang, N.; Johnson, M. A.; DiRisio, R. J.; McCoy, A. B.; Yu, Q.; Bowman, J. M. Disentangling the Complex Vibrational Mechanics of the Protonated Water Trimer by Rational Control of Its Hydrogen Bonds. J. Phys. Chem. A 2019, 123, 7965–7972.
- (35) Duong, C. H.; Yang, N.; Kelleher, P. J.; Johnson, M. A.; DiRisio, R. J.; McCoy, A. B.; Yu, Q.; Bowman, J. M.; Henderson, B. V.; Jordan, K. D. Tag-Free and Isotopomer-Selective Vibrational Spectroscopy of the Cryogenically Cooled H₉O₄⁺ Cation with Two-Color, IR–IR Double-Resonance Photoexcitation: Isolating the Spectral Signature of a Single OH Group in the Hydronium Ion Core. J. Phys. Chem A 2018, 122, 9275–9284.

- (36) Partridge, H.; Schwenke, D. W. The Determination of an Accurate Isotope Dependent Potential Energy Surface for Water from Extensive ab Initio Calculations and Experimental Data. J. Chem. Phys. 1997, 106, 4618–4639.
- (37) Petit, A.; McCoy, A. B. Diffusion Monte Carlo Approaches for Evaluating Rotationally Excited States of Symmetric Top Molecules: Application to H₃O⁺ and D₃O⁺. *J. Phys. Chem. A* **2009**, *113*, 12706–12714.
- (38) McCoy, A. B.; Huang, X.; Carter, S.; Landeweer, M. Y.; Bowman, J. M. Full-Dimensional Vibrational Calculations for H₅O₂⁺ Using an *ab initio* Potential Energy Surface. J. Chem. Phys. **2005**, 122, 061101.
- (39) Mallory, J. D.; Mandelshtam, V. A. Diffusion Monte Carlo Studies of MB-pol (H₂O)₂₋₆ and (D₂O)₂₋₆ Clusters: Structures and Binding Energies. J. Chem. Phys. 2016, 145, 064308.
- (40) Wolke, C. T.; Fournier, J. A.; Dzugan, L. C.; Fagiani, M. R.; Odbadrakh, T. T.; Knorke, H.; Jordan, K. D.; McCoy, A. B.; Asmis, K. R.; Johnson, M. A. Spectroscopic Snapshots of the Proton-Transfer Mechanism in Water. Science 2016, 354, 1131–1135.
- (41) Boyer, M. A.; Chiu, C. S.; McDonald, D. C.; Wagner, J. P.; Colley, J. E.; Orr, D. S.; Duncan, M. A.; McCoy, A. B. The Role of Tunneling in the Spectra of H₅⁺ and D₅⁺ up to 7300 cm⁻⁻¹. J. Phys. Chem. A 2020, 124, 4427–4439.
- (42) Schreiner, P. R.; Kim, S. J.; Schaefer, I., H. F.; Schleyer, P. v. R. M. CH₅⁺: The Never-Ending Story or the Final Word? *J. Chem. Phys.* **1993**, *99*, 3716–3720.
- (43) Mallory, J. D.; Mandelshtam, V. A. Binding Energies From Diffusion Monte Carlo for the MB-pol H₂O and D₂O dimer: A Comparison to Experimental Values. J. Chem. Phys. 2015, 143, 144303.

- (44) Fagiani, M. R.; Knorke, H.; Esser, T. K.; Heine, N.; Wolke, C. T.; Gewinner, S.; Schöllkopf, W.; Gaigeot, M.-P.; Spezia, R.; Johnson, M. A. et al. Gas Phase Vibrational Spectroscopy of the Protonated Water Pentamer: the Role of Isomers and Nuclear Quantum Effects. Phys. Chem. Chem. Phys. 2016, 18, 26743–26754.
- (45) Asvany, O.; Yamada, K. M. T.; Brünken, S.; Potapov, A.; Schlemmer, S. Experimental Ground-State Combination Differences of CH₅⁺. Science **2015**, 347, 1346–1349.
- (46) Schmiedt, H.; Jensen, P.; Schlemmer, S. Unifying the Rotational and Permutation Symmetry of Nuclear Spin States: Schur-Weyl Duality in Molecular Physics. J. Chem. Phys. 2016, 145, 074301.
- (47) Schmiedt, H.; Jensen, P.; Schlemmer, S. Rotation-Vibration Motion of Extremely Flexible Molecules The Molecular Superrotor. *Chem. Phys. Lett.* **2017**, *672*, 34 46.

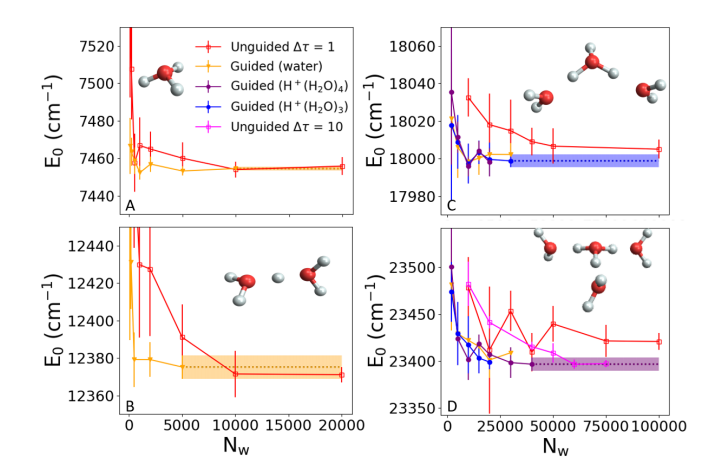


Figure 1: Calculated zero-point energies for (A) H_3O^+ , (B) $H^+(H_2O)_2$, (C) $H^+(H_2O)_3$, (D) $H^+(H_2O)_4$ plotted as functions of the number of walkers used in the simulation. The red or pink symbols and lines provide results of unguided simulations using a 1 a.u. and 10 a.u. time step, respectively. The gold, blue and purple symbols and lines provide results of three types of guided simulations, which are described in the text. The dotted line and shading extends the results of the largest guided simulation in each panel to facilitate comparisons with other calculations. The energies used to generate these plots are also provided in Tables S1-S4.

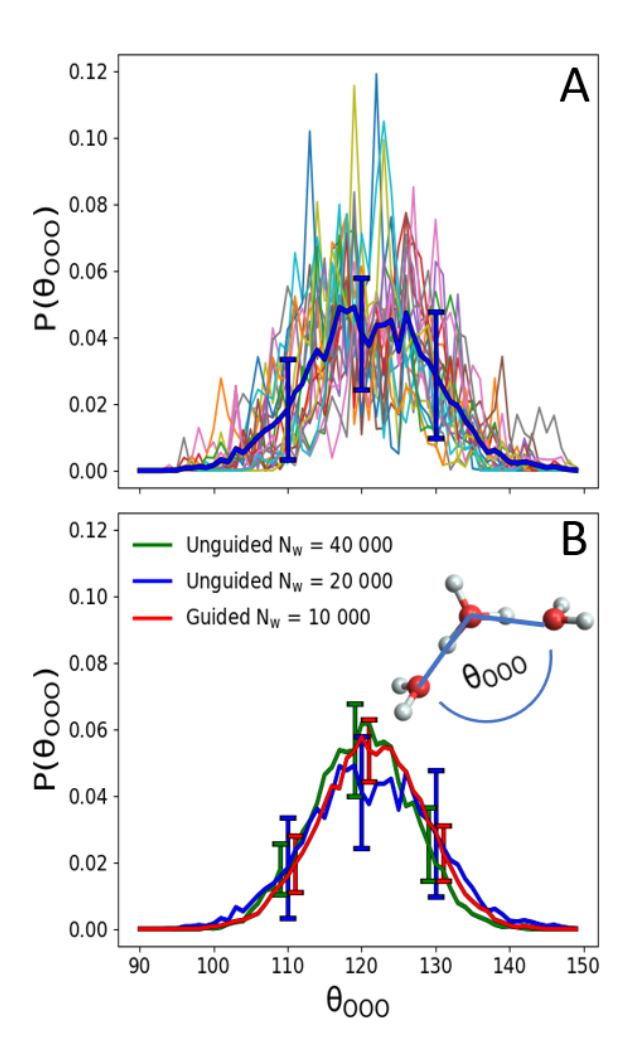


Figure 2: (A) Projections of the ground state probability amplitude for H⁺(H₂O)₃ onto the OOO angle based on the probability amplitudes obtained from 20 DMC wave functions (thin lines). The average of these distributions is plotted with the thick blue line, and the standard deviations at 110°, 120° and 130° are represented by error bars. These results are based on an unguided simulation with 20 000 walkers. (B) Comparison of the average of the projected probability amplitudes based on twenty DMC wave functions obtained from unguided DMC simulations with 20 000 walkers (blue) and 40 000 walkers (green). In addition the projected probability amplitude obtained from a guided DMC simulation with 10 000 walkers is shown in red. For the guided calculation, the guiding function is based on the OH stretches of the outer water molecules and unbound OH bonds in the hydronium core as well as the HOH bends in the outer water molecules. The individual probability distributions used to obtain the green and red curves in panel B are shown in Figure S1.

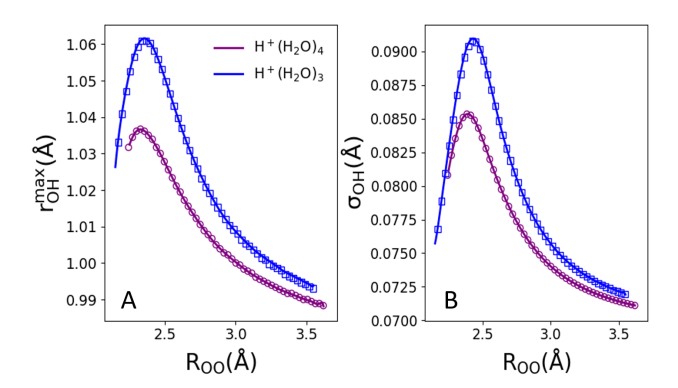


Figure 3: The maximum (A) and width (B) of the ground state wave functions for a water bound OH bond in the hydronium core of $H^+(H_2O)_3$ (blue curves) and $H^+(H_2O)_4$ (purple curves) are plotted as functions of the distance between the oxygen atoms in the hydronium core and the bound water molecule. The curves provide a (n-1)th order polynomial representation of the n data points that are plotted. Additional details about how these values are obtained and the raw data that is plotted are provided in the Supporting Information.

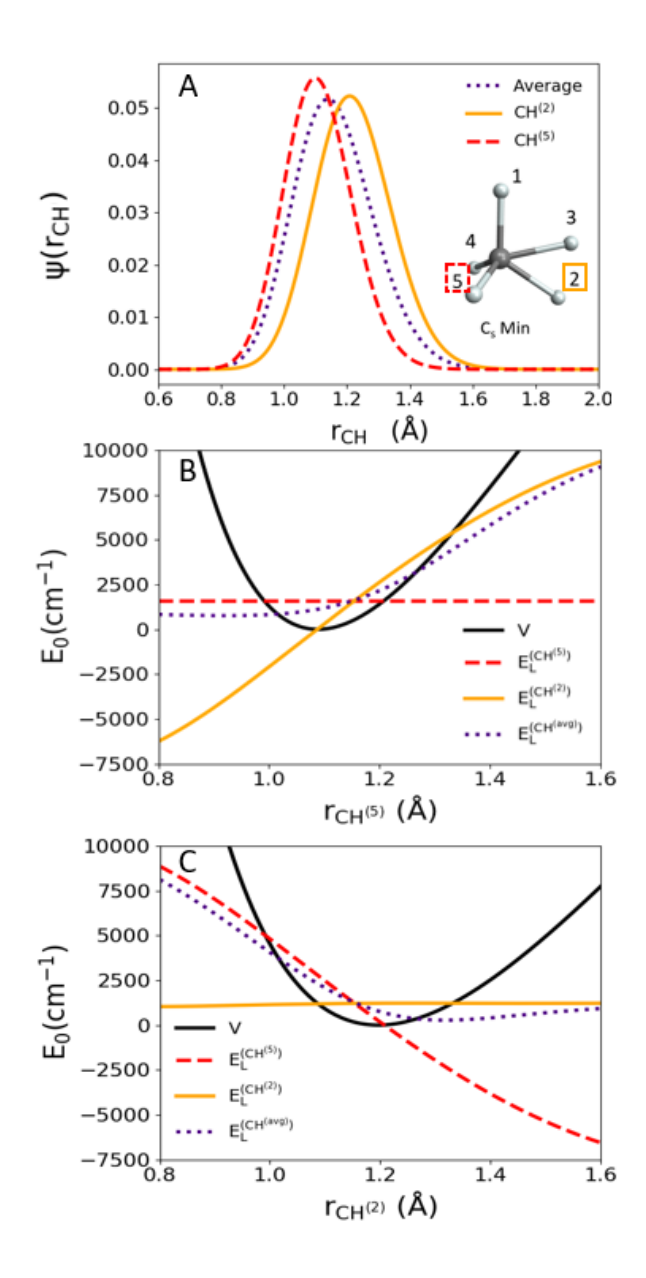


Figure 4: (A) Wave functions for the longest and shortest CH bonds in CH_5^+ (gold solid and red dashed line) as well as the average of the ground state wave functions for the five CH bonds (purple dotted line). (B and C) Local energies obtained from one-dimensional calculations using the potential along (B) $r_{\mathrm{CH}}^{(5)}$ and (C) $r_{\mathrm{CH}}^{(2)}$ (black line) based on the three wave functions shown in panel A.

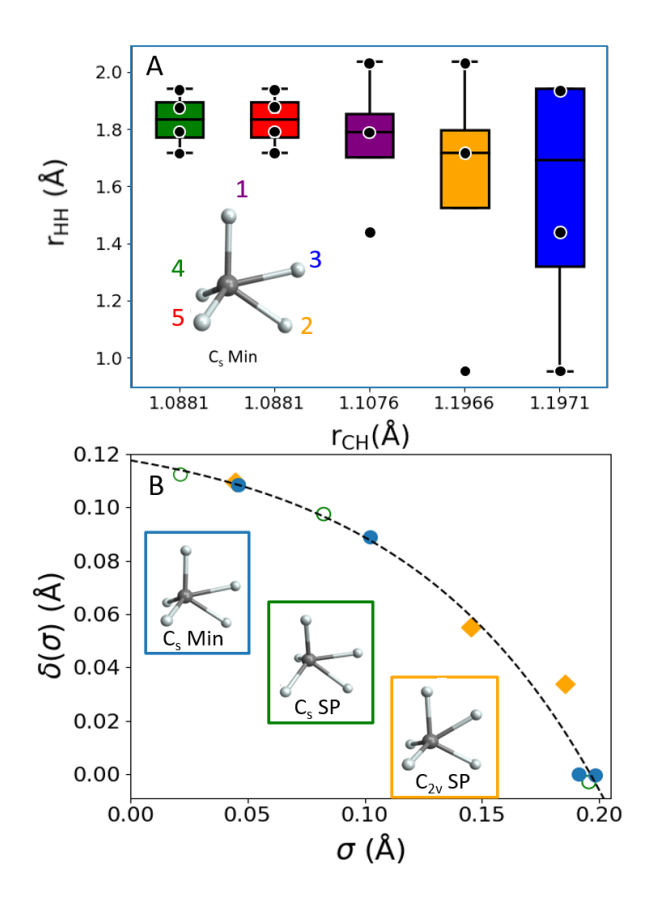


Figure 5: (A) Box and whisker plot showing the standard deviation of H-H distances for each of the five CH bonds on CH_5^+ , plotted as a function of the CH bond length for the equilibrium structure of CH_5^+ . (B) Plot of the displacement of the CH bond length from the value of $r_{CH}^{(2)}$ in the equilibrium geometry of CH_5^+ , δ , as a function of standard deviation of the H-H distances to the hydrogen atom of interest σ , which is also plotted in panel A. These results are plotted for each of the three low-energy stationary point structures of CH_5^+ , shown in the insets. The values for the C_s minimum are plotted with blue filled circles, the values for the C_s saddle point are plotted with green open circles, while the values for the C_{2v} saddle point are shown with filled gold diamonds. The dotted line provides a fit of these values to an exponential function of the form $\delta(\sigma_i) = \text{Aexp}(B\sigma_i) + C$. A, B, and C are -0.02389 Å, 6.29099 Å⁻¹, and 0.24620 Å respectively.

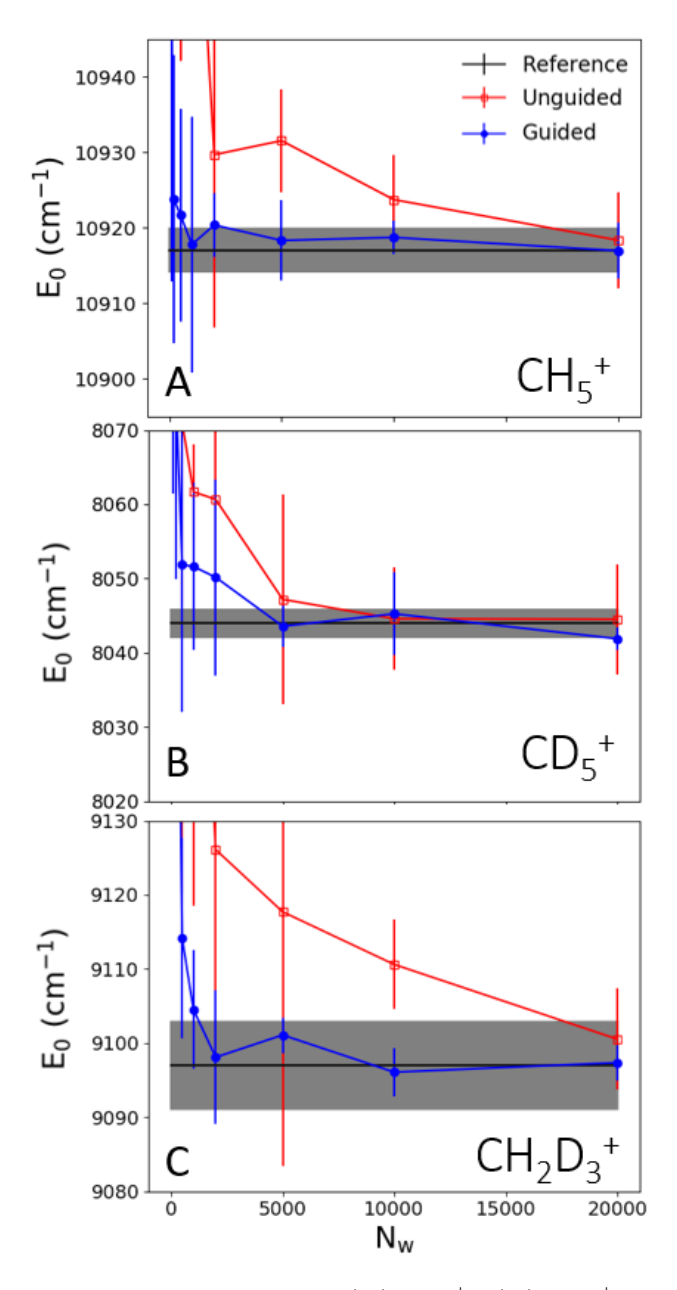


Figure 6: Calculated zero-point energies for (A) CH_5^+ , (B) CD_5^+ , and (C) $\mathrm{CH}_2\mathrm{D}_3^+$ plotted as a function of the number of walkers used in the simulation (N_W) for unguided (blue) and guided (red) DMC simulations. The black lines are the previously reported values of these zero-point energies, and the grey shading indicates their reported uncertainties. ¹⁹ The energies used to generate these plots are also provided in Table S9.

TOC graphic:

